Lawrence Berkeley National Laboratory
Recent Work

Title
Disposition of mullite and mullite-like coatingson silicon carbide by dual-source metal plasma immersion

Permalink
https://escholarship.org/uc/item/9g77q47f

Author
Brown, Ian G.

Publication Date
1997-04-01

eScholarship.org Powered by the California Digital Library
University of California

LBNL-40190
UC-404
ORNL/Sub94-SS109V/02

*DEPOSITION OF MULLITE AND MULLITE-LIKE COATINGS ON SILICON CARBIDE BY DUAL-SOURCE METAL PLASMA IMMERSION**

Topical Report: October '95 through September '96

April 1997

Report prepared by
Ian G. Brown and Othon R. Monteiro
Ernest Orlando Lawrence Berkeley National Laboratory
University of California
Berkeley, CA 94720
under
Memo P.O. 10X-SS109V/02, WBS LBL-2

for

OAK RIDGE NATIONAL LABORATORY
Oak Ridge, Tennessee 37831
Managed by
LOCKHEED MARTIN ENERGY RESEARCH CORP.
for the
U.S. DEPARTMENT OF ENERGY
under contract DE-AC05-96OR22464

*This work was supported by the U.S. Department of Energy, Office of Advanced Resea
Fossil Energy, under Contract Number DE-AC03-76SF00098.

| REFERENCE COPY |
| Does Not |
| Circulate |
Bldg. 50 Library - Ref.
Lawrence Berkeley National Laboratory
Copy 1
LBNL-40190

This report has been reproduced directly from the best available copy.

Available to DOE and DOE contractors from the Office of Scientific and Technical Information, P.O. Box 62, Oak Ridge, TN 37831; prices available from (423) 576-8401.

Available to the public from the National Technical Information Service, U.S. Department of Commerce, 5285 Port Royal Rd., Springfield, VA 22161.

This report was prepared as an account of work sponsored by an agency of the United States Government. Neither the United States Government nor any agency thereof, nor any of their employees, makes any warranty, expressed or implied, or assumes any legal liability or responsibility for the accuracy, completeness, or usefulness of any information, apparatus, product, or process disclosed, or represents that its use would not infringe privately owned rights. Reference herein to any specific commercial product, process, or service by trade name, trademark, manufacturer, or otherwise, does not necessarily constitute or imply its endorsement, recommendation, or favoring by the United States Government or any agency thereof. The views and opinions of authors expressed herein do not necessarily state or reflect those of the United States Government or any agency thereof.

DISCLAIMER

This document was prepared as an account of work sponsored by the United States Government. While this document is believed to contain correct information, neither the United States Government nor any agency thereof, nor the Regents of the University of California, nor any of their employees, makes any warranty, express or implied, or assumes any legal responsibility for the accuracy, completeness, or usefulness of any information, apparatus, product, or process disclosed, or represents that its use would not infringe privately owned rights. Reference herein to any specific commercial product, process, or service by its trade name, trademark, manufacturer, or otherwise, does not necessarily constitute or imply its endorsement, recommendation, or favoring by the United States Government or any agency thereof, or the Regents of the University of California. The views and opinions of authors expressed herein do not necessarily state or reflect those of the United States Government or any agency thereof or the Regents of the University of California.

LBNL-40190
UC-404
ORNL/Sub94-SS109V/02

*DEPOSITION OF MULLITE AND MULLITE-LIKE COATINGS ON SILICON CARBIDE BY DUAL-SOURCE METAL PLASMA IMMERSION**

Topical Report: October '95 through September '96

April 1997

Research sponsored by the U.S. Department ofEnergy,
Office of Fossil Energy
Advanced Research and Technology Development materials program

Report prepared by
Ian G. Brown and Othon R. Monteiro
Ernest Orlando Lawrence Berkeley National Laboratory
University of California
Berkeley, CA 94720

under
Memo P.O. 10X-SS109V/02, WBS LBL-2

for

OAK RIDGE NATIONAL LABORATORY
Oak Ridge, Tennessee 37831
Managed by
LOCKHEED MARTIN ENERGY RESEARCH CORP.
for the
U.S. DEPARTMENT OF ENERGY
under contract DE-AC05-96OR22464

*This work was supported by the U.S. Department of Energy, Office of Advanced Research, Fossil Energy, under Contract Number DE-AC03-76SF00098.

Recycled Paper

Deposition of Mullite and Mullite-like Coatings on Silicon Carbide by Dual-Source Metal Plasma Immersion

Memo P.O. 10X-SS109V/02, WBS Element LBL-2

Principal Investigator: Ian Brown
Co-Investigator: Othon Monteiro

Institution: Lawrence Berkeley National Laboratory
University of California
Berkeley, CA 94720

Project Period: October '95 through September '96

SUMMARY

Mullite and mullite-like coatings on silicon carbide have been produced by a Metal Plasma Immersion Ion Implantation and Deposition (Mepiiid) technique based on two cathodic vacuum arc sources and concurrent pulse biasing of the substrate in an oxygen atmosphere. The deposition was carried out at oxygen partial pressures of between 0.66 and 3.33 Pa. The Al:Si ratio in the films varied from 1:1 to 8:1 and was controlled by varying the pulse duration of the separate plasma guns. High bias voltage was used early in the deposition process in order to produce atomic mixing at the film-substrate interface, while lower bias voltage was used later in the deposition; low ion energy allows control of the physical properties of the film as well as faster deposition rates. The as-deposited films were amorphous, and crystalline mullite was formed by subsequent annealing at 1100°C for 2 hours in air. Strong adhesion between the mullite and the SiC was achieved, in some cases exceeding the 70 MPa instrumental limit of our pull-tester.

Research sponsored by the U.S. Department of Energy, Fossil Energy Advanced Research and Technology Development Materials Program, DOE/FE AA 15 10 10 0, Work Breakdown Structure Element LBL-2.

I. INTRODUCTION

The properties of silicon carbide make it an outstanding material for use in high temperature applications in harsh environments. Among the properties of technological importance are its high mechanical strength at both room and elevated temperatures, high thermal conductivity, low thermal expansion coefficient, high temperature stability and high oxidation resistance[1,2]. Because of its combined high mechanical strength and high thermal conductivity, SiC also has a very good resistance to thermal shock.

Studies using thermal gravimetric analysis and direct microscopic observations[2,3] have demonstrated that noticeable oxidation of SiC starts at temperatures above 820°C and becomes more severe in the presence of moisture in high temperature environments. Amorphous SiO_2 is the main solid product of the oxidation in this temperature range. As the oxidation temperature increases beyond 1200°C, α-SiO_2 (crystoballite) becomes the prevalent solid product[2,3], and the adhesion between the allotropic forms of silicon dioxide and silicon carbide is diminished because of the mismatch in the thermal expansion coefficients of silicon carbide and the crystalline oxides.

In order to increase the chemical stability of SiC at elevated temperatures, mullite ($3Al_2O_3.2SiO_2$) is an attractive coating material[3-5]. Mullite has good resistance to oxidizing and reducing high temperature environments, good mechanical properties at high and low temperatures, and a coefficient of thermal expansion (CTE) close to that of SiC. The use of substrate and coatings with similar CTEs minimizes thermal stresses generated during high temperature cycling, and therefore decrease the chances of delamination.

Among the techniques investigated for deposition of mullite on silicon carbide, conventional plasma spray[5] has been shown to produce films that can crack and debond from the substrate; in this case delamination results from an amorphous aluminum-silicon oxide phase at the coating-substrate interface. Plasma spray succeeds in depositing well-adhered mullite films when the substrate is maintained at a temperature greater than the recrystallization temperature of mullite, i.e. above about 1050 °C. Chemical vapor deposition has also been investigated for forming mullite coatings[6,7]. In one CVD approach, alumina and silica layers were alternately deposited and the resulting multilayer structure annealed in an attempt to form mullite by interdiffusion. However, the large mismatch in coefficients of thermal expansion and embrittlement of the crystallized silica resulted in failure of the coating during the annealing treatment. Another CVD approach uses direct formation of mullite via CVD by co-deposition of Al and Si oxides[7] at elevated temperatures.

We have investigated the deposition of aluminum-silicon oxides using a vacuum arc based technique in which metal plasmas are formed and mixed in an oxygen atmosphere. The technique has previously been used to deposit a variety of oxides, such as Al_2O_3 coatings on iron-aluminides using a single source of aluminum plasma in a low pressure oxygen background[8]. The method has several advantages over other approaches: (a) it allows deposition of silicon-aluminum oxides with a wide range of compositions, that of stoichiometric mullite being just one of them, (b) the co-deposition promotes close physical mixture of the Si and Al atoms, and therefore long range diffusion of Si and Al during the recrystallization of the amorphous film into mullite is not necessary, minimizing the possibility of failures due to phase separation, (c) there is no need for toxic or hazardous chemicals such as chlorides or others, (d) it allows deposition at both low and high temperatures.

II. EXPERIMENTAL

A. Plasma Processing

The method used here for the deposition of mullite films is a vacuum arc plasma synthesis approach. The vacuum arc is a high current discharge between two electrodes in vacuum in which metal plasma is produced in abundance[9,10]. For the work described here we used small, repetitively-pulsed vacuum arc plasma guns operated at a pulse duration of about 5 ms and repetition rate about 1 Hz, and arc current in the range 100 – 300 A. Along with the metal plasma that is generated, a flux of macroscopic droplets ranging from 0.1 - 10 mm in diameter is also produced[9-12]. In general it is desirable to remove the solid particulate contamination and this was done using a curved 'magnetic duct' which stops line-of-sight transmission of macroparticles while allowing the transport of plasma[13,14]. The overall plasma deposition system thus consists of the repetitively pulsed plasma gun in conjunction with a 90° bent magnetic filter. Plasma exits the filter and deposits onto the appropriately positioned substrate.

Oxides are formed by carrying out the deposition not in a high vacuum environment but in a somewhat higher pressure of oxygen; we have found empirically that a pressure in the range 0.1 - 10 Pa is suitable for most purposes. At pressures above about 10 Pa the growth rates is substantially decreased, whereas at pressures much below 0.1 Pa oxygen deficient oxides are often produced. In the present work the oxygen background pressure was varied between about 0.5 and 5 Pa. The oxygen is both entrained in the plasma stream, ionized, and deposited, as well as reacts with the freshly-deposited metallic surface to form aluminum oxide or silicon dioxide; the latter process dominates. The substrate temperature is estimated to be below 100°C for the SiC coupons were mounted on a directly water cooled substrate holder.

Ion energy of the depositing plasma flux is controlled by repetitively pulse biasing the substrate. Pulsing of the bias voltage is necessary (for all but the lowest bias voltages) because a high-voltage dc bias would cause an electrical discharge between the substrate and the vessel or the plasma gun; the plasma would be grossly perturbed (because the plasma sheath would expand from the substrate to large distances). The solution is to switch off the bias before a discharge can occur (to limit the sheath expansion to modest distances), let the plasma recover, and then repeat the process; i.e., to do the biasing in a repetitively pulsed mode. The fraction of time that the voltage is applied is defined as duty cycle, and typically the pulse duration might be ~10 μs and the duty cycle ~10 - 50%. For the early stages of the deposition process the pulse bias (V_{bias}) is held at a relatively high voltage of -2.0 kV. The mean aluminum ion energy (E_i) is then 3.4 keV, because the mean ion charge state (Q) of the aluminum plasma is 1.7 and $E_i = QV_{bias}$; for silicon the mean charge state is 1.4 and the mean ion energy 2.8 keV; (the charge state spectra of vacuum arc produced plasmas have been discussed in detail in refs. 15,16). At this energy ions are implanted into the substrate to a depth of up to ~100 Å. The film thus grows on the SiC substrate from a highly mixed interface. When a film thickness of just a few tens of angstroms has accumulated, the pulse bias voltage is reduced, since intermixing with the substrate is no longer a factor and the higher ion energy would sputter away the already-deposited film. For the bulk of the plasma deposition process the pulse amplitude is kept at -200 volts.

A simplified schematic of the overall dual-gun system consisting of the two plasma guns and macroparticle filters, which were used in this investigation is shown in Figure 1, and a photograph of the mixing plasmas is shown in Figure 2.

B. Film deposition

In the deposition procedure used here, we have combined the plasma streams from two separate plasma sources, one with an aluminum-silicon alloy cathode with the Al:Si ratio being 3:1, and the other consisting of pure silicon. The plasma guns were triggered simultaneously and the ratio between Al and Si in the film was controlled by varying the duration of the plasma pulse (arc duration). The deposition rate produced by each individual source was determined (in terms of nanometers per pulse) as a function of oxygen partial pressure by measuring the thickness of the deposited film after a certain number of arc pulses of well-defined duration. Based on an assumed value of molar volume of the film, a deposition rate in terms of deposited metal atoms per arc pulse was estimated for each source. Films of desired compositions were then produced. In all experiments the pulse duration was such that the deposition rate was less 0.1 nm per pulse, thus enhancing the homogeneity and preventing stratification of the films.

C. Silicon carbide

Two different grades of silicon carbide were used as substrates for the deposition of the films throughout this study. The one used in almost all of the experiments has the following composition: 94.4% SiC, 3% Al, 2% C, and 0.6% B. This particular material was sintered at the Lawrence Berkeley National Laboratory's (LBNL) Materials Science Division, and the Al, C and B were added as sintering aids. Two slightly different processing routes of this material, which resulted in large differences in electrical resistivities, were used. Density of the sintered material was 99% of theoretical. In addition to this silicon carbide, a commercial grade (Hexolloy 5) from Carborundum Industries was also used in few depositions. In all cases the surface of the silicon carbide was ground and polished to a mirror finish prior to deposition.

D. Characterization techniques

Film thickness was measured using a Tencor Alpha-Step profilometer. These measurements were used for calibration of the deposition rates from the individual plasma sources so as to achieve the desired stoichiometry, as described in Section B above. Scanning electron microscopy was carried out with a JEOL SEM Model 6400 to characterize the surface morphology of uncoated SiC and the coated samples before and after heat treatments. At 30kV accelerating voltage surface charging was not severe enough to require conductive coating of the samples.

The oxygen, aluminum and silicon contents in the amorphous films were determined by Rutherford backscattering spectrometry using 1.8 MeV He^{+} ions. Although the technique is suitable for determining the Al and Si contents, the RBS-determined oxygen content is subject to some uncertainty as discussed in the Results section, below.

X-ray diffraction was extensively used to characterize the structure of the films deposited on the SiC substrates before and after heat treatment. X-ray diffractograms were obtained in a SIEMENS D-500 diffractometer using Cu K_a radiation in a glancing-angle configuration. Scans were performed at 40 kV and 30 mA from 20° to 70° with a step size of 0.02° and a speed of $0.01^{\circ}s^{-1}$. Data processing such as smoothing and background removal was performed by a standard commercial software package.

Transmission electron microscopy of the deposited films was performed using a JEOL 200CX microscope. Specimens from the as-deposited films were prepared by placing a NaCl crystal adjacent to the SiC during the oxide deposition in the vacuum chamber. The oxide film was then floated off the NaCl crystal in a 50% (by volume) methanol-water solution, and the film placed immediately on a copper (100 mesh) grid. The role of the alcohol was to decrease the surface tension of the water, and therefore allow thinner films to be handled without damaging them. The advantage of this method is that it avoids any need for further sample preparation such as ion milling or chemical etching, which may result in artifacts.

Adhesion tests of the as-deposited and annealed films were conducted with a Sebastian-type pull-tester built in-house. Because this is not a standardized test the results were (and should be) used only for comparison among the several tests performed here, in particular, the effect of the post-deposition heat treatment. In this test, an aluminum pin is epoxy-glued to the surface of a coated SiC coupon, and a normal load is applied to pull the pin away from the coupon. The load at which separation occurs is recorded and converted to an equivalent stress. The upper limit of this test is determined by the strength of the glue used, which in our case corresponds to a stress of about 70 MPa.

E. Annealing

After deposition, the coated samples were annealed at 1100°C for two hours in air. The purpose of this annealing was to investigate the formation of crystalline mullite from the amorphous oxide films with a large range of Al:Si ratios, as well as any other crystalline phase. In addition this annealing allowed a first evaluation of any degradation that may occur in the film or at the interface upon exposure to elevated temperatures in air.

III. RESULTS AND DISCUSSION

The silica-alumina binary phase diagram[17] indicates that the only stable phase other than Al_2O_3 and SiO_2 is mullite, whose composition ranges from approximately $3Al_2O_3.2SiO_2$ to $2Al_2O_3.SiO_2$. The mullite structure consists basically of octahedral AlO_6 chains parallel to the c-axis and cross linked by tetrahedral $(Al,Si)O_4$ chains[18]. The exact content of Al and Si in mullite has been reported to lie in a composition range wider than that suggested by the phase diagram[18,19], and the fine detail of its real structure is still subject to controversy [18-20].

A scanning electron micrograph of the polished surface of an uncoated piece of LBNL silicon carbide is shown in Figure 3a. The SiC grains are noticeably elongated, which increases the mechanical properties of the material; other significant features observed in the micrograph are the presence of small quantities of a second phase, resulting from the sintering additives, and some porosity. Figure 3b shows an SEM image of the LBNL SiC after being coated with the aluminum-silicon oxide film using conditions #1 described in Table I. The grain morphology is not seen anymore, but some (near-)circular features have apparently been formed during the deposition. These features will be shown later in this report to consist of voids.

Our initial attempts at forming mullite films on SiC consisted of using a single plasma source with an aluminum-silicon cathode with Al:Si atomic concentration of 3:1. Films deposited at various oxygen partial pressures using the single cathode approach resulted in coatings with a

composition substantially different from that of the cathode, with the Al:Si ratio about three times higher than that in the original cathode, as can be seen from the results shown in Table I, sample sets #4 and #5. Two main reasons can account for such a discrepancy: differences in rates of Al and Si plasma formation at the cathode, and differences in Al and Si ion concentrations (distribution) in the transported plasma stream due to differences in mass and charge of the ions.

Analysis of the composition of the cathode surface prior to and after a coating experiment, as well as analysis of the film deposited using the single source, have demonstrated that the major reason for the differentiated concentration resulted from cathode phenomena. Elemental analysis of the cathode by RBS indicated that the Al:Si ratio prior to deposition was in fact 3:1. After deposition of a 200 nm thick film, the surface of the cathode was analyzed again, as well as the film composition. The Al:Si ratios were 2:1 and 8:1 respectively, confirming that the difference between the composition of the film and the cathode material is due in large part to a different rate of plasma formation for the Al and Si elements. The enrichment of Al in the film and corresponding enrichment of Si on the cathode surface can be explained by taking into consideration the difference in melting points of the two elements. The maximum solubility of Si in Al is 1.6% (weight) and the solubility of Al in Si is even lower, and therefore the cathode with Al:Si ratio 3:1 consisted actually of a mixture of two phases: aluminum with a small silicon content, and silicon with virtually no aluminum[21]. In bi-phase materials the arc root tends to be located at the lower melting point phase, and therefore the plasma is in general enriched somewhat with the elements from this phase[9].

In order to produce films with the correct Al:Si ratio, we decided to introduce a second plasma source, with a silicon cathode. In order to be able to obtain a particular stoichiometry in the films, the deposition rate from each gun had to be determined, as well as the composition of the film produced by each individual gun. Under a set of standard deposition conditions, the deposition rates of the aluminum-silicon oxide and the silicon oxide were 0.15 and 0.05 nm per 5 ms arc pulse respectively. The Al:Si ratio in the deposited film was around 8:1 (see for instance Table I, depositions #4 and #5). In computing the length of the individual pulses needed to achieve the desired stoichiometry, both the composition resulting from each source and the deposition rate were taken into account.

A remark is due at this point with regard to the choice of cathodes that we used for synthesizing the mullite films. There is no intrinsic reason that prevented us from doing the same experiments with one aluminum cathode and one silicon cathode, instead of with one cathode made of Al:Si and other of Si. The former approach, in fact, would be simpler than the latter, and would allow for a better composition uniformity as a function of depth. The choice made in this study to use one cathode made of Al(3):Si(1) alloy and the other of pure silicon resulted from the fact that at the beginning of this investigation we were attempting to produce mullite films solely with the Al(3)-Si(1) alloy, and then chose to use a second Si gun so as to correct for the Si deficiency.

Based on the estimated deposition rates, several sets of films were produced. The experimental conditions for each individual set are shown in Table I – the duration of the plasma pulses and the background oxygen pressure in the deposition vessel. Films of aluminum-silicon oxides were produced with Al:Si ratios near that of stoichiometric mullite, and significantly above and below that. The compositions of the oxide films resulting from such depositions, as measured by RBS, are also included in Table I. Uncertainties in the Al and Si content are of the order of 15%.

The oxygen content in these films measured by RBS is also shown in Table I. Since oxygen is lighter than the other two elements, the uncertainty in its concentration is of 20%. The amount of oxygen was higher than that corresponding to mixtures of ordinary alumina and silica when deposition was carried out at pressures of 3.3 Pa. Assuming that the oxide films consist of mixtures of Al_2O_3 and SiO_2, oxygen contents in sets #1, #2, and #3 in Table I would be 8.6, 12.1 and 3.8 respectively. These values are all lower than the measured values, suggesting an oxygen enrichment with respect to the equilibrium stoichiometry.

The excess oxygen is likely to result from oxygen atoms initially at the oxide surface being implanted by knock-on collisions with incoming energetic aluminum and silicon ions. At the deposition pressures used in this investigation the time required to adsorb a monolayer of oxygen on the growing surface is of the order of 0.1 ms, which corresponds to an arrival rate substantially higher than the arrival rate of aluminum or silicon ions at the growing surface. Since the oxidation rate of freshly deposited aluminum and silicon in this environment is high, we expect that complete oxidation of freshly deposited metal occurs as the film grows. Direct oxidation of the deposited Al and Si would only account for the stoichiometric forms of Al_2O_3 - SiO_2, i.e. with no excess oxygen with respect to a silica - alumina mixture. However, in addition to the surface oxidation, recoil implantation of the adsorbed oxygen resulting from collisions with the incoming energetic plasma ions could then lead to the observed high values of oxygen concentration Another cause for the high oxygen content is direct implantation of oxygen ions by the pulse-bias voltage applied to the substrate. Oxygen ions may be produced in the plasma, although the degree of oxygen ionization is expected to be low. A direct comparison between the compositions of the films produced in runs#4 and #5 show that there is a direct correlation between the oxygen partial pressure and the oxygen content of the films. The recoil implantation mechanism alone is not capable to account for this correlation, since it is difficult to justify the a differentiated implantation between Al and O. (A similar effect occurs for Si and O also, of course). Therefore oxygen ionization should not be disregarded.

An edge-on SEM image of a sample from set #6 after it has been annealed at 1100°C in air is shown in Figure 4(a), and indicates the integrity and uniformity of the mullite film. Figure 4(b) shows another area of the same sample, with a bubble-like feature under the mullite coating. These bubble-like defects tend to be a few microns in diameter, and therefore much greater than the film thickness, and are located just below the deposited film. Such defects were found in several samples prior to the annealing treatment, and their origin is discussed later in this paper. An X-ray diffraction pattern of the aluminum-silicon oxide films from deposition #1 before annealing is shown in Figure 5. The as-deposited films were basically amorphous. The diffraction patterns of a series of films after annealing are shown in Figure 6 where several peaks characteristic of mullite in addition to those of the silicon carbide can be seen, as indicated. The low intensity of the mullite diffraction peaks is mostly due to the small film thickness. Another silicon-aluminum oxide known as sillimanite (Al_2SiO_5) also provides a reasonable fit to the peaks in the diffractogram, but it was discarded because the ratio of the intensities of the diffraction peaks was closer to that expected from mullite.

The X-ray diffraction patterns of films #1 through #5 after annealing suggested that in this composition range there was virtually no difference among the annealed films. In all cases, the only new crystalline phase observed, which was not present before annealing, was mullite. The absence of diffraction peaks from other phases was somewhat unexpected, particularly in the Al rich films. In the films with very low Al:Si ratio (e.g. sample #3, which was clearly out of the

stability domain of mullite according to the Al_2O_3-SiO_2 phase diagram) the excess silicon was expected to form silicon dioxide upon high temperature annealing, which being amorphous would not contribute any peaks to the diffractogram. Amorphous silica does not recrystallize into crystoballite at temperatures below 1200°C, and therefore may be present in the coating without being detected. At the other extreme, i.e. in films with very high Al:Si ratio, peaks from crystalline alumina were expected because the recrystallization temperature of alumina is below 1100°C, and again the Al:Si ratio in the film was outside the mullite domain. No alumina peaks were detected. Two probable reasons may account for the absence of alumina peaks in the films: mullite may form during high temperature annealing by the reaction between the excess aluminum oxide and silicon from the silicon carbide, therefore consuming all the excess aluminum that might otherwise form crystalline alumina; or the excess Al may still be accommodated in the mullite structure, resulting only in small lattice parameter changes. There have been references in the literature to mullite with a wide range of compositions, including Al:Si ratios as high as 9:1[19,20,22]. The lattice parameter a of mullite has been shown to vary continuously with the aluminum oxide content in the mullite[19]. The diffractograms in Figure 6 do not have enough resolution to discriminate between the small changes in lattice parameters that would result even for large changes in the Al content in the mullite. The different alumina content in the mullite may affect of the actual performance of the coating at high temperature. This effect has not been studied yet.

The presence of amorphous silica in mullite films deposited in SiC can be undesirable. It has been reported that excess silicon in amorphous mullite films can result in phase separation of amorphous silica during the recrystallization of the mullite[5]. This glassy silica may account for a premature failure of the coating upon thermal cycling because of the local differences in the CTE. Similarly, the precipitation of alumina may also be detrimental for resistance of the coating to thermal shock.

Transmission electron diffraction of the as-deposited films also indicates, in agreement with the X-ray results, that the films are predominantly amorphous. Figure 7(a) shows a selected area diffraction pattern from an as-deposited mullite film produced using conditions #1 (Table I). The majority of the thin films observed by TEM have this type of diffraction pattern. Some indication of crystalline mullite present in the thicker areas of the free-standing film was also observed, as is indicated by the diffraction pattern shown in Figure 7(b), where one can see the superposition of diffuse rings from an amorphous phase and a single crystal spot pattern, which has been indexed as a <001> zone axis of mullite. Since the recrystallization temperature of mullite is high (between 700°C and 1000°C)[5,19], it is very improbable that their temperature reached such values. Thermal spikes may have occurred locally, raising the film temperature to levels where crystalline mullite can form.

Adhesion tests of the as-deposited and annealed films were performed and the results are shown in Table II. Some uncertainty in these results can be expected from local variations in the microstructure of the substrate, the coating, or in the epoxy itself, although multiple measurements can reduce the uncertainty. The adhesion values presented are the result of three measurements (the uncertainty is typically about ±5 MPa), and there is a clear indication of substantial enhancement in adhesion strength after annealing. This increase may be due to solid state reactions and/or diffusion that takes place during the high temperature treatment. The instrumental limit of the pull-test is around 70 MPa, above which the epoxy that joins the pin to the coated SiC fails.

In the SiC samples used in experiments #1 through #5, some microstructural features that resemble micro-bubbles were observed immediately after the deposition, and persisted after annealing at 1100°C. SEM images of annealed sample #4 after the adhesion test clearly show these bubbles: Figure 8(a) is from an area which still has the film intact, and the bubbles look like circular areas of dark contrast, whereas Figure 8(b) is from an area originally underneath the pin, i.e. from a region that had the coating removed, and therefore has the SiC exposed. The voids are easily seen, suggesting that these voids were at the silicon carbide - oxide interface. A careful observation of the cross section of the sample shown in Figure 4(b) allows the observation of such voids underneath the coating. The presence of micro-bubbles is expected to facilitate delamination of the coatings due to the reduction of actual interface area, or alternatively weakening the SiC itself near the interface, and therefore it is imperative that their occurrence be minimized, if not eliminated.

In order to eliminate the presence of bubbles, it is necessary to understand the mechanism responsible for their formation. A tentative explanation is given below. Bubbles, when present, are formed during the deposition process and not during the high temperature annealing, and therefore their presence cannot be explained by the formation of carbon dioxide during the high temperature annealing treatments.

One possible reason for the observed "bubble phenomenon" could be electric breakdown within the SiC substrate. Dielectric breakdown in insulators usually takes place in localized channels that experience high electric field and therefore high current. During the actual breakdown, high temperature gradients are established around the breakdown channels. This initiates an interdiffusion flux of the lightest component species into the areas of highest temperature and a diffusion of the heaviest species toward the periphery of the channels, resulting in a carbon enrichment in the channels. The free carbon atoms then diffuse toward the free surface due to the high temperature and high pressure in the channels. In fact silicon carbide breakdown and void formation, very similar to that seen here, has been observed during diamond deposition in the presence of an applied bias voltage[23]. In the early stages of oxide film deposition, high bias voltage is applied to the substrate to promote atomic mixing at the film-substrate interface and thereby enhance the film-substrate adhesion. If the high voltage is sufficient to achieve electric breakdown in the SiC then bubble-like defects may form.

Two other types of silicon carbide with electrical resistivities different from those used in experiments #1 through #6 were used as substrates for mullite deposition in order to determine whether the density of micro-bubbles would change. The first type consisted of a SiC prepared at LBNL, similar to that used previously, but that had been subjected to a different final processing step. This change led to a significant increase in electrical resistivity (about one order of magnitude). The other type of SiC used was the commercially available Hexolloy (by Carborundum Industries). When the same deposition conditions described in runs #1 through #5 in Table I were used to deposit a mullite film on these SiC substrates, no bubbles were found, and the adhesion tests resulted in higher values as shown in Table III. The increased adhesion can be interpreted as resulting from the absence of defects at the SiC/oxide interface. The absence of bubbles when the deposition was carried out on SiC with high resistivities supports the idea that the micro-bubbles are linked to electrical phenomena during the deposition.

IV. CONCLUSIONS

We have synthesized highly-adherent mullite and mullite-like films on silicon carbide using a novel plasma-based method in which aluminum and silicon plasma streams are mixed in an oxygen background and deposited while a repetitively-pulsed bias voltage is applied to the substrate so as to control the ion energy during deposition. A relatively high bias voltage (i.e., high ion energy) is used in the early stages of the deposition so as to enhance the adhesion via atomic mixing at the interface, while a lower bias voltage (ion energy) is used during the bulk of the deposition so as to provide an "ion beam assist" to the growing film surface for the production of good film structure.

Amorphous aluminum-silicon oxide films with a wide range of Al:Si ratio were produced by this technique by controlling the duration of the separate plasma pulses. Upon annealing of the deposited films, mullite was the only detected crystalline phase, irrespective of the Al:Si ratio in the as-deposited film. The adhesion strength between the mullite film and the SiC substrate after high temperature annealing was at or near 70 MPa, the instrumental limit of measurement.

The adhesion of the mullite films is affected by the bias voltage, which promotes atomic mixing at the interface, and the interface morphology, which may or may not have a high density of voids. The presence of micro-bubbles at the interface reduces the strength of the adhesion between the silicon carbide and the mullite films, and these bubbles appear to be linked to the electrical properties of the SiC and its interaction with the deposition parameters. The presence of voids at the interface can be minimized by preventing electric breakdown of the silicon carbide during the bias voltage application. In order to maximize adhesion, the deposition process and the substrate should be such that a bubble-free interface is formed.

ACKNOWLEDGMENTS

We would like to express our appreciation to Kin Yu for providing the RBS measurements, to Peggy Hou for the high temperature annealing, and to Bob MacGill and Mike Dickinson for their support of the experimental equipment. We are grateful for Marie-Paule Delplanke-Ogletree for valuable discussions and critical comments. The electron microscopy part of this work was conducted at the National Center for Electron Microscopy, which is supported by the Director, Office of Energy Research, Office of Basic Energy Sciences, Materials Science Division, U.S. Department of Energy. This work was supported by the U.S. DOE, Office of Advanced Research, Fossil Energy, under subcontract to Oak Ridge National Laboratory 10X-SS109V, WBS Element LBL-2.

REFERENCES

1. P. Shaffer, "Engineering Properties of Carbides", in *Engineered Materials Handbook, Vol. 4: Ceramics and Glasses* (ASM International, Metal park, OH, 1991), pp. 804-811.
2. N.S. Jacobson, J. Am. Ceramic Soc. **76**, 3 (1993).
3. E.L. Courtright, Surf. and Coatings Technol. **68/69,** 116 (1994).
4. J.R. Price and M. van Roade, Ceram. Trans. **10**, 469 (1990).
5. K.N. Lee, R A. Miller and N.S. Jacobson, J. Am. Ceramic Soc. **78,** 705 (1995).
6. R.P. Mulpuri and V K. Sarin, "Mullite Coatings for Corrosion Protection of Silicon Carbide", Proc. 9th. Annual Conf. on Fossil Energy Materials, Knoxville, TN. 1995 (Pub. Conf. 9505204, pub. U.S. DOER); p. 85.
7. R.P. Mulpuri and V K. Sarin, J. Mat. Res. **11**, 1315 (1996).
8. O R. Monteiro, Z. Wang , K.-M. Yu , P.Y. Hou, I.G. Brown, B.H. Rabin and G.F. Kessinger, in *Plasma Deposition of High Temperature Protective Coatings*, Oak Ridge, TN, 1996.
9. J.M. Lafferty, *Vacuum Arcs - Theory and Applications* (Wiley, New York, 1980).
10. R.L. Boxman, P. Martin and D. Sanders, *Vacuum Arc Science and Technology* (Noyes, New York, 1995).
11. J.E. Daalder, Physica **104C,** 91 (1981).
12. D.T. Tuma, C.L. Chen and D.K. Davies, J. Appl. Phys. **49,** 3821 (1978).
13. I.I. Aksenov, A.N. Belokhvostikov, V G. Padalka, N.S. Repalov and V.M. Khoroshikh, Plasma Phys. and Controlled Fusion **28,** 761 (1986).
14. A. Anders, S. Anders and I.G. Brown, Plasma Sources Sci. and Technol. **4,** 1 (1995).
15. I.G. Brown and X. Godechot, IEEE Trans. Plasma Sci. **PS-19,** 713 (1991).
16. I.G. Brown, Rev. Sci. Instrum. **10,** 3061 (1994).
17. I.A. Aksay and J.A. Pask, J. Am. Ceramic Soc. **58,** 507 (1975).
18. T. Epicier, M.A. O'Keefe and G. Thomas, Acta Crystallographica **A46,** 948 (1990).
19. R.X. Fisher, H. Schneider and D. Voll, J. European Ceramic Soc.**16,** 109 (1996).
20. S.H. Rahman, S. Strohenk, C. Paulmann and U. Feustel, J. European Ceramic Soc. **16,** 177 (1996).
21. *ASM Handbook: Alloy Phase Diagrams*; Vol. 3, edited by H. Baker (ASM International, 1994).
22. T. Ban and K. Okada, J. Am. Ceramic Soc. **75,** 227 (1992).
23. M. Ibn-Charaa, M. Jaouen, J. Delafond and L. Pranevicius, Diam. Related Mat. **5,** 128 (1996).

Table I: Deposition conditions, film composition and thickness of the as-deposited aluminum-silicon oxide films produced by dual-source Mepiiid

Deposition	Al-Si Pulse	Si Pulse	Pressure		Content		Thickness
	(ms)	(ms)	(Pa)	Al	Si	O	(nm)
#1	5	5	3.3	4.4	1	10.4	240
#2	5	2.5	3.3	6.7	1	16	230
#3	5	10	3.3	1.2	1	5.3	240
#4	5	0	3.3	8	1	19.5	220
#5	5	0	0.6	7.4	1	13	240
#6	5	5	3.3				2000
Mullite				3	1	6.5	

Table II: Adhesion of aluminum-silicon oxide films on silicon carbide prior to and after annealing in air for 2 h at 1100°C

Deposition	Adhesion as-deposited (MPa)	Adhesion annealed (MPa)	Content Al	Content Si	Content O	Thickness (nm)
#1	35	70	4.4	1	10.4	240
#2	38	57	6.7	1	16	230
#3	31	63	1.2	1	5.3	240
#4	31	57	8	1	19.5	220
#5	20	65	7.4	1	13	240

Table III: Adhesion of as-deposited aluminum-silicon oxide films on high resistivity silicon carbide.

Deposition	Al:Si Pulse (ms)	Si Pulse (ms)	P (Pa)	Adhesion as-deposited (MPa)
#7	5	5	6.6	59
#9	5	0	6.6	70

Figure Captions

Figure 1: Schematic diagram of the dual-gun plasma immersion deposition system used during metal plasma immersion ion-implantation and deposition of aluminum-silicon oxides.

Figure 2: Photograph of actual plasma streams in the dual-gun plasma immersion system. The plasma streams are bent by the magnetic field generated by the coils in order to prevent the incidence of macroparticles on the substrate.

Figure 3: Scanning electron micrograph of (a) polished surface of uncoated silicon carbide prepared at LBNL; and (b) as deposited aluminum-silicon oxide film on SiC done at conditions #1 in Table I.

Figure 4: (a) Edge-on scanning electron microscope image of annealed mullite film from sample set #6 in Table I.
(b) Image of another area of the same sample, where a micro-bubble like defect (about 10mm in size) is indicated by the arrow.

Figure 5: X-ray diffraction pattern of the aluminum-silicon oxide films from deposition #1 prior to heat treatment. The peaks identified with an S are from silicon carbide.

Figure 6: X-ray diffraction patterns of the aluminum silicon oxide films produced with a range of Al:Si ratios, after annealing at $1100^{o}C$ for 2 hours in air. The Al:Si ratio in each of the films are also noted in the Figure.

Figure 7: Selected area transmission electron diffraction pattern from a as-deposited silicon-aluminum oxide deposited under conditions #1 (Table I). (a) Diffuse rings labeled A indicate amorphous phase, predominates across the film (b) Spot pattern of mullite in the zone axis <001> sporadically found in the thicker regions of the specimen

Figure 8: Scanning electron micrograph of SiC coated with aluminum silicon oxide film deposited at conditions #1 in Table I after annealing at $1100^{o}C$ for 2 hours in air. (a) shows area where the film is still intact; (b) shows area where the film was removed during the pull test.

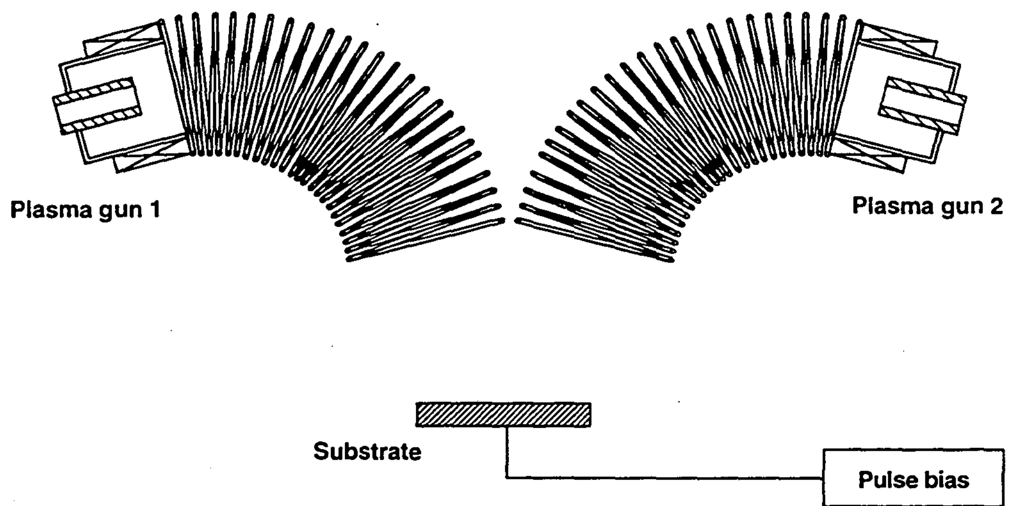

Figure 1

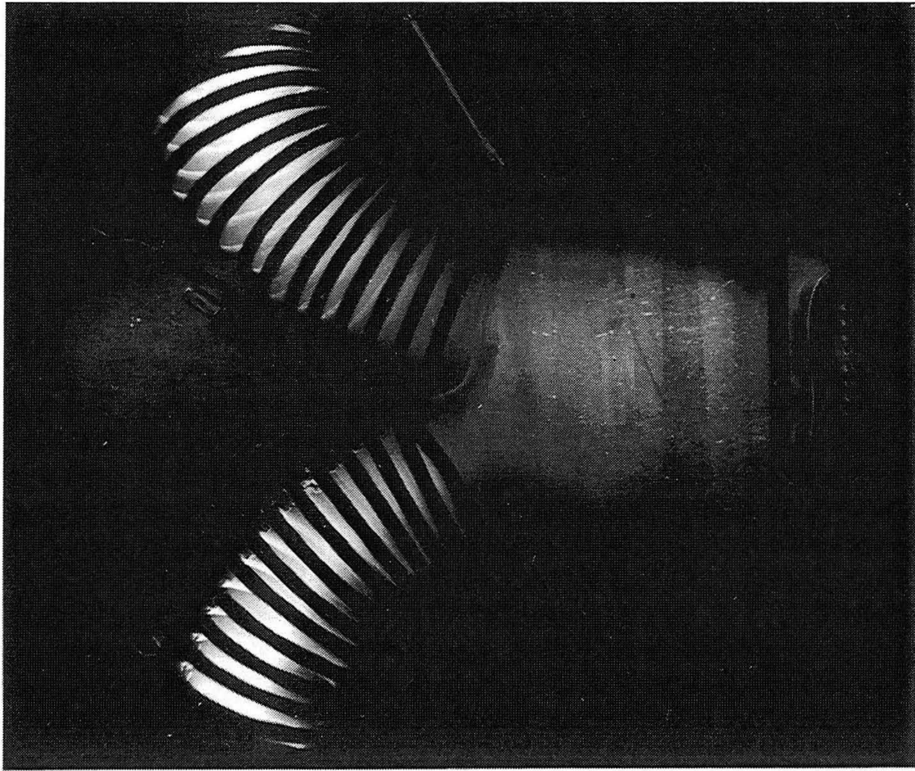

Figure 2

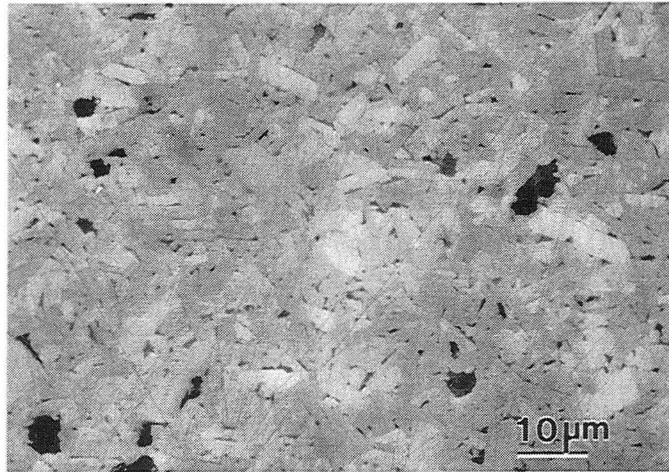

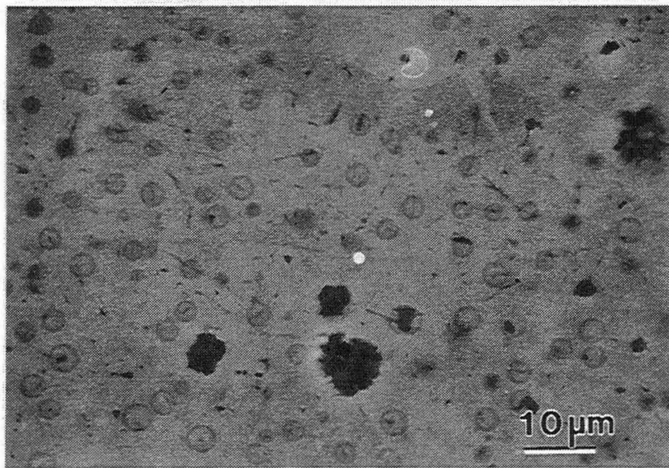

Figure 3(a) and 3(b)

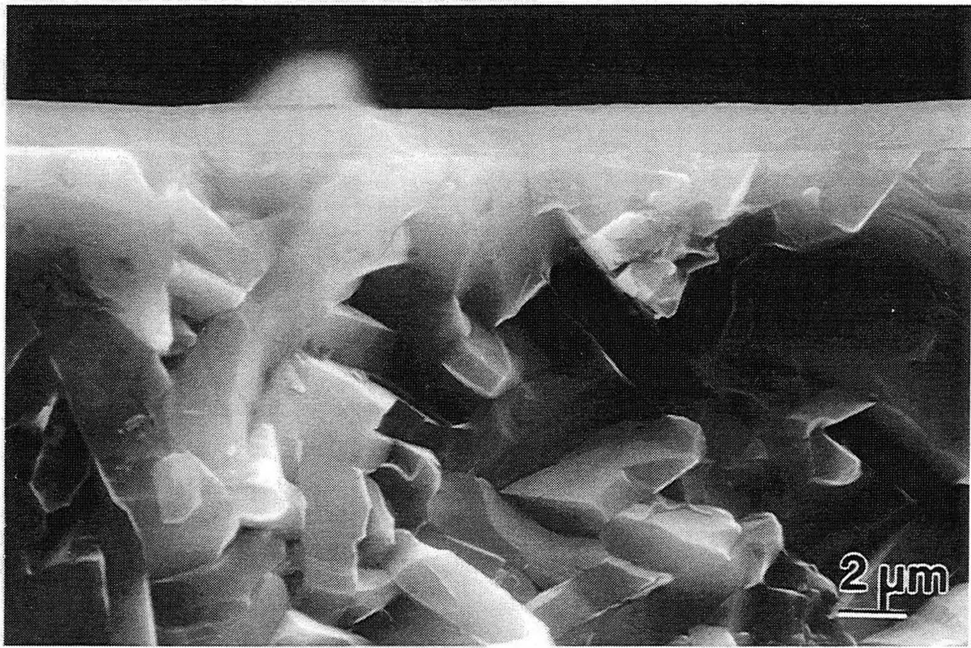

Figure 4(a)

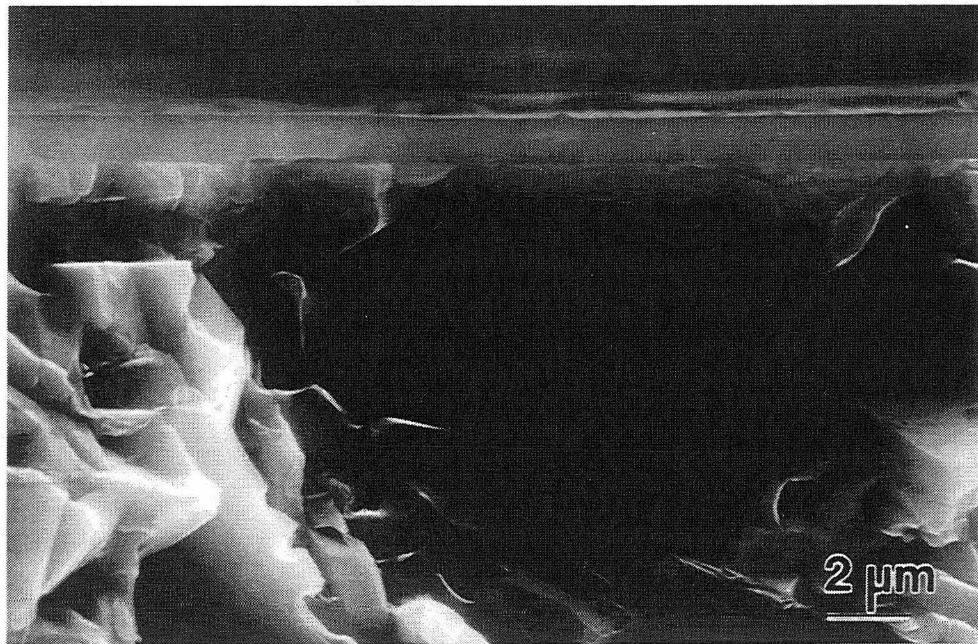

Figure 4(b)

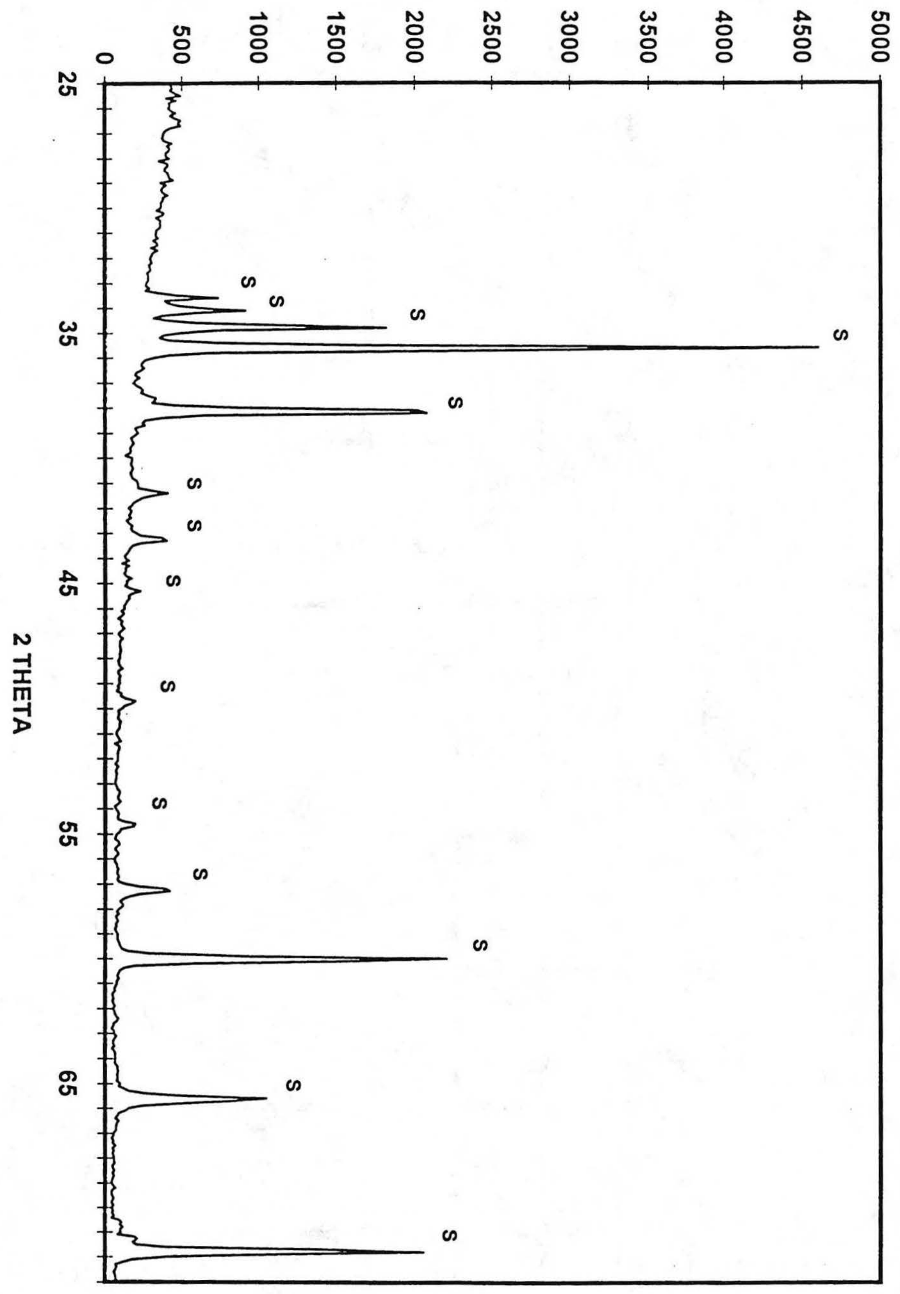

Figure 5

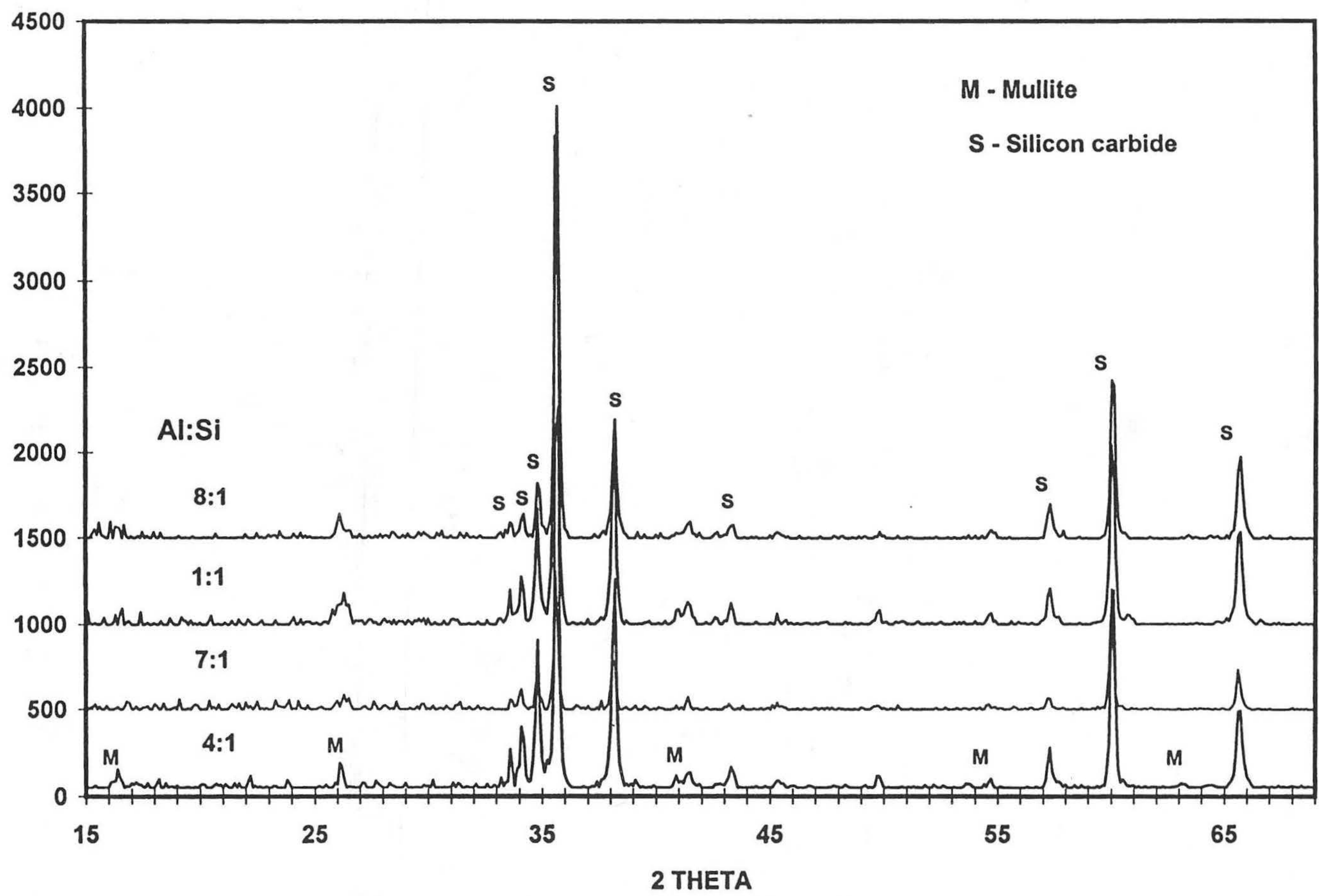

Figure 6

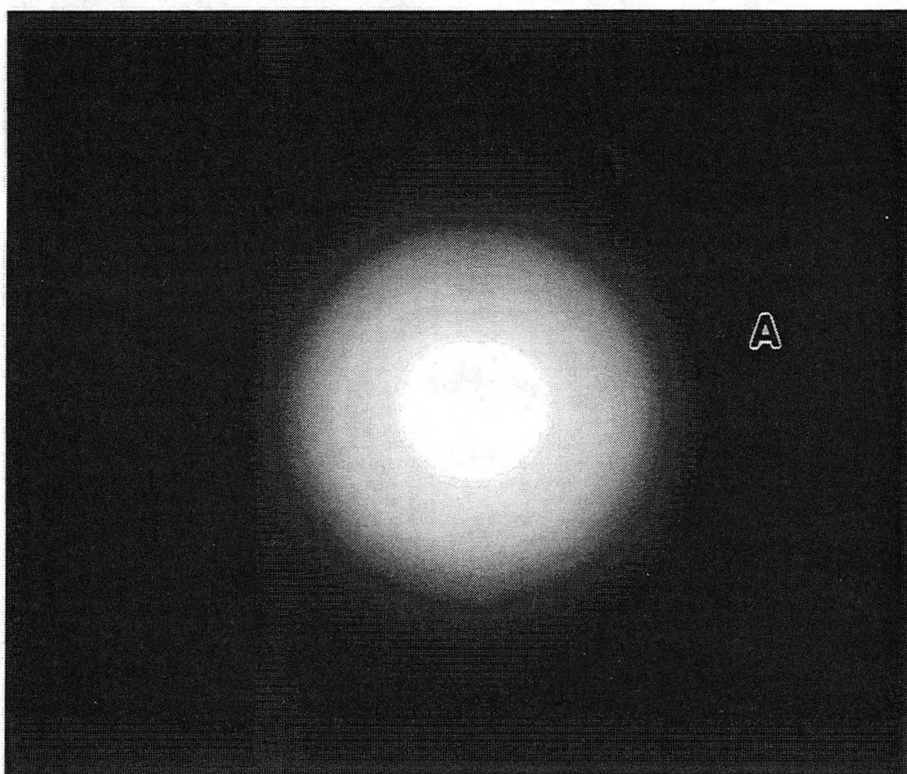

Figure 7(a)

Figure 7(b)

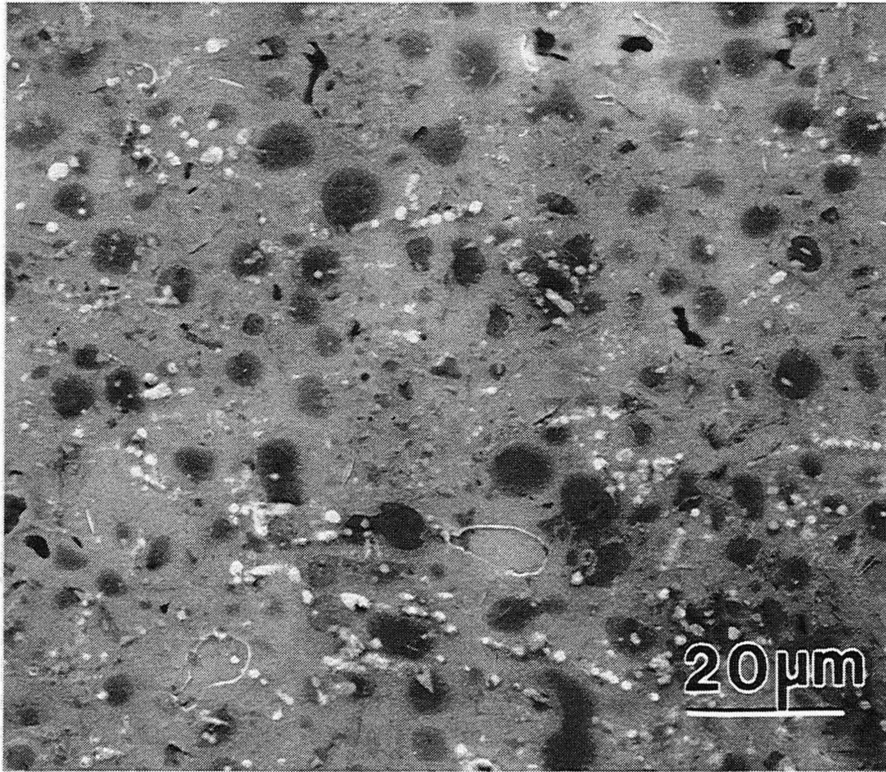

Figure 8(a)

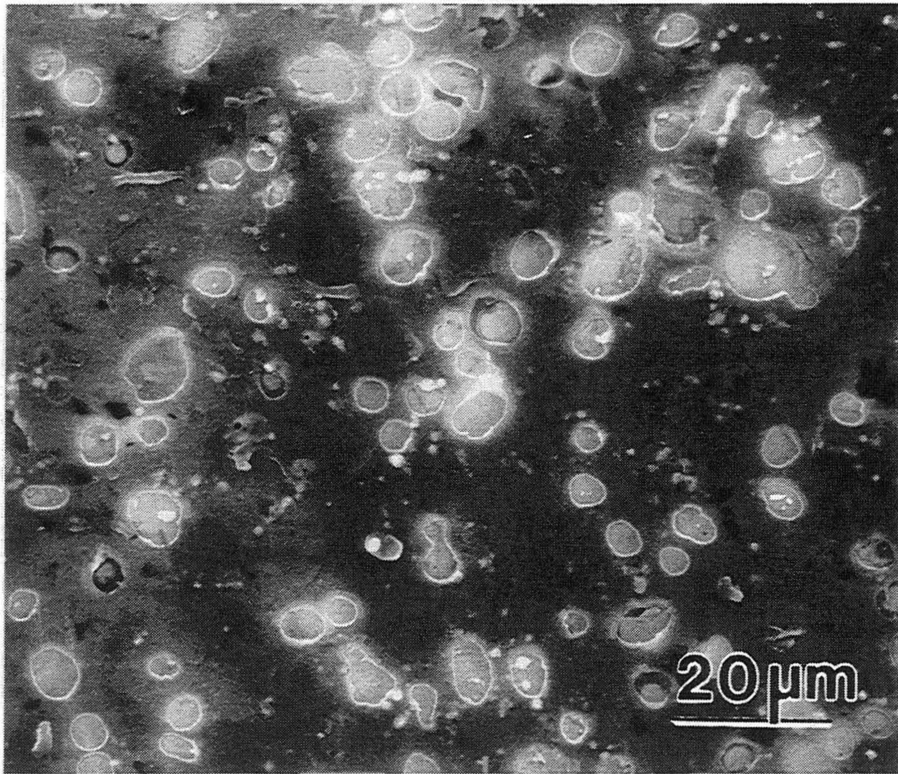

Figure 8(b)

CORROSION DISTRIBUTION

AIR PRODUCTS AND CHEMICALS
P.O. Box 538
Allentown, PA 18105
S. W. Dean

ALBERTA RESEARCH COUNCIL
Oil Sands Research Department
P.O. Box 8330
Postal Station F
Edmonton, Alberta
Canada T6H5X2
L. G. S. Gray

ALLISON GAS TURBINE DIVISION
P.O. Box 420
Indianapolis, IN 46206-0420
P. Khandelwal (Speed Code W-5)
R. A. Wenglarz (Speed Code W-16)

ARGONNE NATIONAL LABORATORY
9700 S. Cass Avenue
Argonne, IL 60439
K. Natesan

ARGONNE NATIONAL LABORATORY-WEST
P.O. Box 2528
Idaho Falls, ID 83403-2528
S. P. Henslee

BABCOCK & WILCOX
Domestic Fossil Operations
20 South Van Buren Avenue
Barberton, OH 44023
M. Gold

BRITISH COAL CORPORATION
Coal Technology Development Division
Stoke Orchard, Cheltenham
Glocestershire, England GL52 4ZG
J. Oakey

CANADA CENTER FOR MINERAL & ENERGY TECHNOLOGY
568 Booth Street
Ottawa, Ontario
Canada K1A OG1
R. Winston Revie
Mahi Sahoo

DOE
DOE OAK RIDGE OPERATIONS
P. O. Box 2001
Oak Ridge, TN 37831
Assistant Manager for Energy Research and Development

DOE
DOE OAK RIDGE OPERATIONS
P. O. Box 2008
Building 4500N, MS 6269
Oak Ridge, TN 37831
M. H. Rawlins

DOE
MORGANTOWN ENERGY TECHNOLOGY CENTER
P.O. Box 880
Morgantown, WV 26505
R. C. Bedick
D. C. Cicero
F. W. Crouse, Jr.
N. T. Holcombe
W. J. Huber
J. E. Notestein

DOE
OFFICE OF FOSSIL ENERGY
FE-72
19901 Germantown Road
Germantown, MD 20874-1290
F. M. Glaser

DOE
OFFICE OF BASIC ENERGY SCIENCES
Materials Sciences Division
ER-131, GTN
Washington, DC 20545
H. M. Kerch

DOE
PITTSBURGH ENERGY TECHNOLOGY CENTER
P.O. Box 10940
Pittsburgh, PA 15236
A. L. Baldwin
G. V. McGurl
T. M. Torkos

ELECTRIC POWER RESEARCH INSTITUTE
P.O. Box 10412
3412 Hillview Avenue
Palo Alto, CA 94303
W. T. Bakker
J. Stringer

EUROPEAN COMMUNITIES JOINT RESEARCH CENTRE
Petten Establishment
P.O. Box 2
1755 ZG Petten
The Netherlands
M. Van de Voorde

FOSTER WHEELER DEVELOPMENT CORPORATION
Materials Technology Department
John Blizard Research Center
12 Peach Tree Hill Road
Livingston, NJ 07039
J. L. Blough

IDAHO NATIONAL ENGINEERING LABORATORY
P. O. Box 1625
Idaho Falls, ID 83415
A. B. Denison

LAWRENCE BERKELEY NATIONAL LABORATORY
University of California
Berkeley, CA 94720
Ian Brown

LAWRENCE LIVERMORE NATIONAL LABORATORY
P.O. Box 808, L-325
Livermore, CA 94550
W. A. Steele

LEHIGH UNIVERSITY
Materials Science & Engineering
Whitaker Laboratory
5 E. Packer Avenue
Bethlehem, PA 18015
John N. DuPont

MOBIL RESEARCH & DEVELOPMENT CORPORATION
P. O. Box 1026
Princeton, NJ 08540
R. C. Searles

NATIONAL MATERIALS ADVISORY BOARD
National Research Council
2101 Constitution Avenue
Washington, DC 20418
K. M. Zwilsky

OAK RIDGE NATIONAL LABORATORY
P.O. Box 2008
Oak Ridge, TN
P. T. Carlson
F. D. Johnson **(5 copies)**
R. R. Judkins
D. P. Stinton
P. F. Tortorelli
M. R. Upton
I. G. Wright

RISOE NATIONAL LABORATORY
P.O. Box 49
DK-4000
Roskilde, Denmark
Aksel Olsen

SHELL DEVELOPMENT COMPANY
WTC R-1371
P.O. Box 1380
Houston, TX 77251-1380
W. C. Fort

SOUTHWEST RESEARCH INSTITUTE
6620 Culebra Road
P.O. Drawer 28510
San Antonio, TX 78284
F. F. Lyle, Jr.

TENNESSEE VALLEY AUTHORITY
1101 Market Street
3A Missionary Ridge
Chattanooga, TN 37402-2801
A. M. Manaker

TENNESSEE VALLEY AUTHORITY
Energy Demonstration & Technology
MR 2N58A
Chattanooga, TN 37402-2801
C. M. Huang

THE MATERIALS PROPERTIES COUNCIL, INC.
United Engineering Center
345 E. Forty-Seventh Street
New York, NY 10017
M. Prager

UNIVERSITY OF TENNESSEE AT KNOXVILLE
Materials Science and Engineering
Department
Knoxville, TN 37996
R. A. Buchanan

WESTERN RESEARCH INSTITUTE
365 N. 9th Street
P.O. Box 3395
University Station
Laramie, WY 82071
V. K. Sethi

WESTINGHOUSE ELECTRIC CORPORATION
Research and Development Center
1310 Beulah Road
Pittsburgh, PA 15235
S. C. Singhal

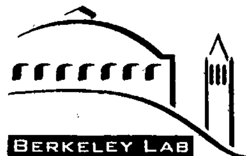

ERNEST ORLANDO LAWRENCE BERKELEY NATIONAL LABORATORY
TECHNICAL AND ELECTRONIC INFORMATION DEPARTMENT
UNIVERSITY OF CALIFORNIA | BERKELEY, CALIFORNIA 94720